

Physical constraints on the design of the DEMO pellet fueling system

B. Pégourié^a, C. Day^b, A. Frattolillo^c, F. Koechl^d, P.T. Lang^e

^(a) IRFM, CEA Cadarache, 13108 Saint-Paul-lez-Durance, France

^(b) Karlsruhe Institute of Technology, 76021 Karlsruhe, Germany

^(c) ENEA C.R. Frascati, 00044 Frascati, Rome, Italy

^(d) Fusion@ÖAW, Atominstitut, TU Wien, Austria

^(e) Max Planck Institute for Plasma Physics, 85748 Garching, Germany

Pellets have demonstrated their capacity for depositing matter in the plasma core and are the best candidates for DEMO fueling. This deep matter deposition results from two phenomena: the pellet penetration which – for given plasma density and temperature profiles – depends on the pellet mass and injection velocity (the ablation phase), then the displacement of the locally deposited material due to its drift down the magnetic field gradient during the homogenization phase. Present day devices and DEMO exhibit very different characteristics with respect to these two phenomena. In today's machines, pellet penetration λ_p is larger than the ∇B -induced displacement Δ ($\Delta/\lambda_p \sim 0.5$ - it is the reason for which it is possible to fuel them efficiently using Low Field Side launched pellets), while in DEMO the matter penetration will be dominated by the ∇B -induced displacement, with typical values of $\Delta/\lambda_p \sim 2-3$. It follows that - for an efficient fueling – it is enough that the pellet penetrates inside $\sim 2a/3$ in present day machines (where a is the plasma minor radius), and mandatory that all the ablation occurs in the High Field Side half of the plasma in DEMO (Figure 1). For this reason, **the fueling of DEMO can be only ensured by pellets injected from the HFS** [1].

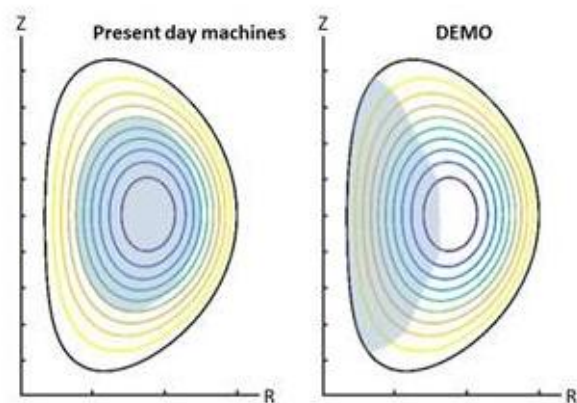


Fig. 1: The optimal pellet penetration region is shown as the shadowed zone.

Constraints on the DEMO pellet fueling system and the resulting design is based on injection simulations with the pellet ablation-deposition code HPI2. The latter – which is valid for any magnetic and plasma configurations - computes the pellet ablation taking into account thermal ions and electrons and the suprathermal ions generated by the plasma heating systems [2]. The drift model is based on the compensation of the cloud polarization by parallel currents [3]. An additional effect is the pre-cooling of the plasma by the previously deposited material

drifting in front of the pellet in the case of HFS injection. Work hypotheses are a pellet particle content identical to that of the ITER pellets ($N_p = 6 \times 10^{21}$ atoms) and an injection velocity compatible with the presently available injector technology ($V_p \leq 1.5-2 \text{ km/s}$). The injection velocity – which is limited due to the use of curved guide tubes in HFS injection configuration – is estimated through the empiric AUG scaling [1]: $V_p [\text{m/s}] = 36.4 \sqrt{R_c / \Phi_p}$, where R_c is the curvature radius and Φ_p the pellet size (the slowing down of the pellet in the guide tube is not taken into account). Most of the calculations were done with a configuration that was used in the 2013/2014 physics assessment, of major and minor radii $R = 9 \text{ m}$ and $a = 2.25 \text{ m}$, on-axis magnetic field $B = 6.6 \text{ T}$, current $I_p = 16.8 \text{ MA}$, average density and electron temperature $\langle n_e \rangle = 9 \times 10^{19} \text{ m}^{-3}$ and $\langle T_e \rangle = 12.9 \text{ keV}$. For each configuration, the deposition profile is characterized by (see Figure 2):

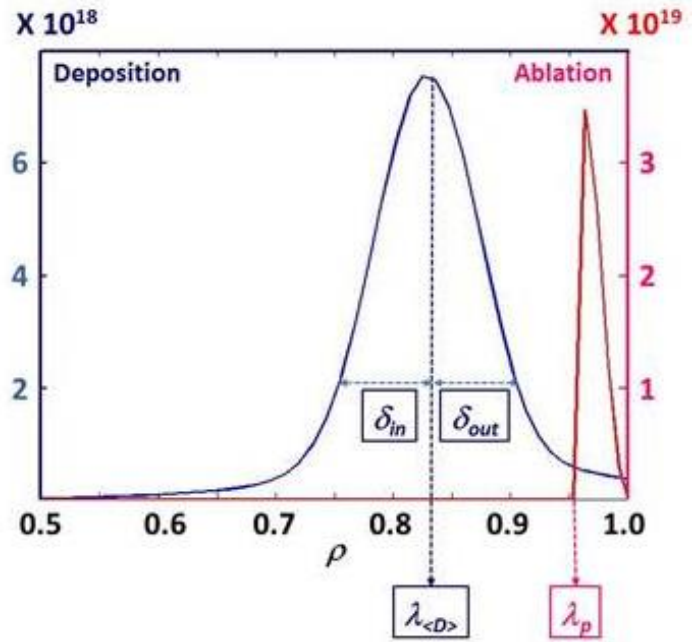


Fig. 2: Characterization of the ablation and deposition profiles.

The radius of the barycenter of the deposition, $\lambda_{(D)}$.

The typical inboard (outboard) width of deposition ($1/e$ of maximum), δ_{in} (δ_{out}).

The radial interval in which the deposition is effective $\Delta_D = [\lambda_{(D)} - \delta_{in}; \lambda_{(D)} + \delta_{out}]$.

For all the simulations presented below, the fueling efficiency $\varepsilon = \frac{4\pi^2 R a}{N_p} \int \rho (n_e^{post} - n_e^{pre}) d\rho$

- where ρ is the normalized minor radius and n_e^{post} and n_e^{pre} the post- and pre-injection densities – is larger than 0.95. However, it must be noted that this definition takes only into account the effect of the ∇B -induced drift, and not that of the triggered ELM. It is therefore only to be taken as an upper boundary.

Pellet penetration in the optimal ablation zone (Fig.1) can be obtained through HFS or Vertical-HFS geometries. In the former case (HFS), the pellet velocity (and thus its penetration) is limited due to the curved guide tube, but the drift – directed along the major radius – is quasi-perpendicular to the flux surfaces and thus of maximum efficiency. In the

latter (VHFS), the velocity is only limited by the injector technology, but the penetration (in term of flux surface) is penalized by the plasma elongation and the drift, in this case almost tangential to the flux surfaces, of low efficiency. A comparison was done, varying the radial R_{inj} (vertical Z_{inj}) position of the injection point for

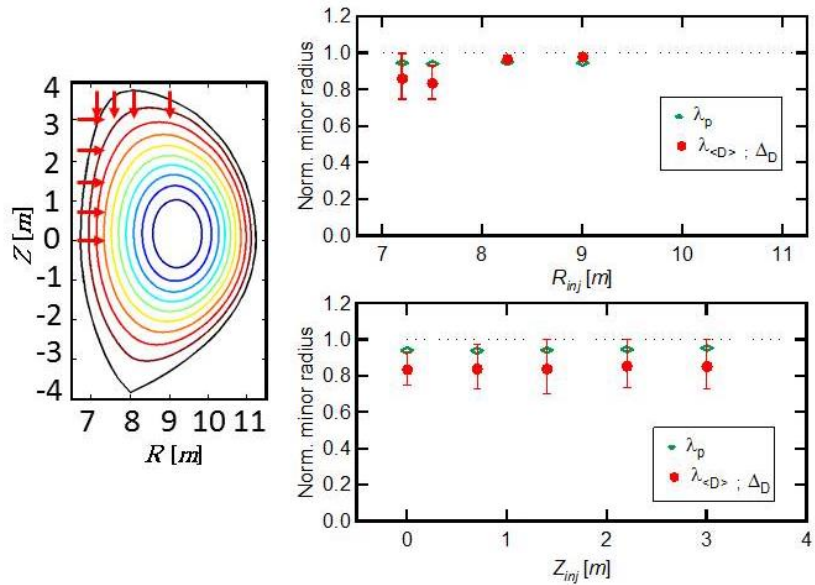


Fig. 3: Investigating the role of different radial (vertical) locations for a VHFS (HFS) pellet launched at 1000 m/s

VHFS (HFS) geometries, and using a pellet velocity $V_p = 1\text{ km/s}$ in all cases (Figure 3). It is seen that significant core deposition is only achieved for launching locations inside $R_{inj} \sim 8\text{ m}$ for VHFS pellets when no significant impact of Z_{inj} on the fueling is observed for HFS pellets. **In general, any VHFS launch location would require a high injection velocity (in the 5-10 km/s range, out of the capacity of present day injectors) for satisfactory performance.**

The independency of the fueling characteristics on the vertical position of the launching point for HFS pellets indicates that the direction of V_p has no importance, provided its component perpendicular to the flux surfaces, V_R , is maximized. For technical constraints, the guide tube exits vertically from the device, parallel to the central solenoid. It follows that the larger the guide tube curvature, the larger V_p , but the smaller the ratio V_R/V_p .

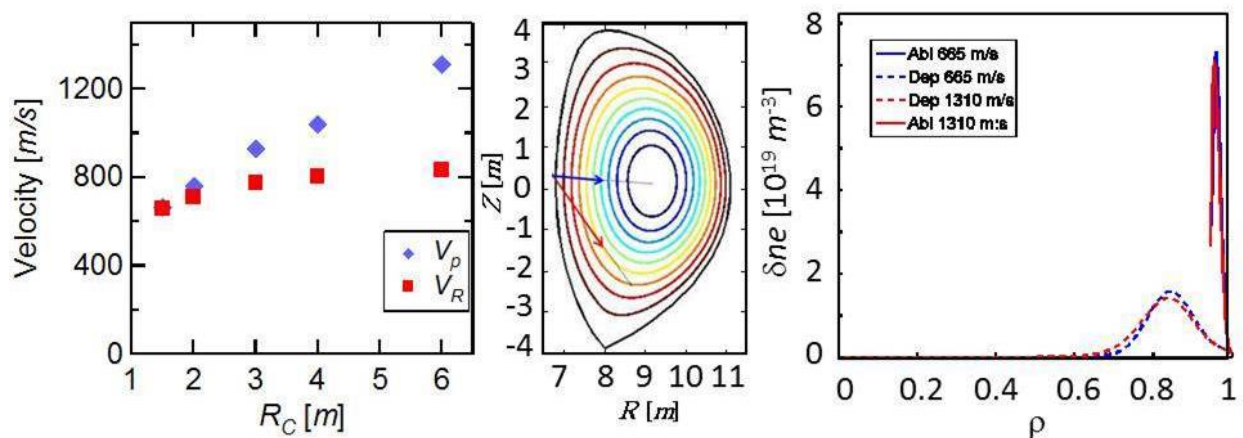


Fig. 4: Dependence on the injection and radial velocities on the curvature radius. Comparison of the deposition profiles for $R_c = 1.5$ and 6 m .

An example is shown in Figure 4, which displays V_p and V_R vs. R_c , and the resulting ablation/deposition profiles for $R_c = 1.5$ and $6m$. It follows from the similarity between the two deposition profiles that the final constraint is essentially the limitation of the pellet erosion in the guide tube. The results reported above show a remarkable insensitivity to many injection and pedestal parameters. **Globally, the best fueling is obtained by HFS injection via a guiding tube of curvature radius $\geq 4m$, launching pellets to enter the separatrix at a vertical position distant by less than $2a/3$ from the horizontal mid plane.**

Following these lines, three injection line options were designed for the most recent DEMO configuration [4]: major and minor radii $R = 9.07m$ and $a = 2.93m$, on-axis magnetic field $B = 5.7T$, current $I_p = 19.6MA$, average density and electron temperature $\langle n_e \rangle = 8 \times 10^{19} m^{-3}$ and $\langle T_e \rangle = 13keV$.

Their design maximizes V_R (line 1), the penetration angle of the pellet in the plasma (line 2), or R_c – and thus V_p (line 3).

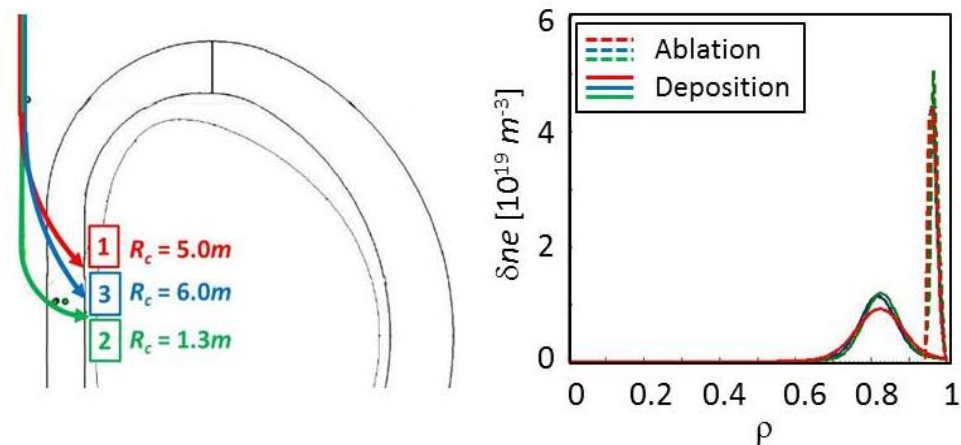


Fig. 5: Design of the DEMO pellet injection lines and corresponding ablation and deposition profiles.

They are displayed in Figure 5, with the corresponding ablation/deposition profiles. **The fueling characteristics are very similar, exhibiting a fueling efficiency $\epsilon > 0.97$ and a deposition centered at $\lambda_{(D)} \sim 0.82$ with a radial extent $\delta_{in/out} = \pm 0.1$.** The criterion for choosing between these three configurations is then the limitation of the stress imposed to the pellet during its transfer and the minimization of the associated mass loss.

[1] P.T. Lang *et al.*, Fusion Eng. Des. **96–97** (2015) 123

[2] B. Pégourié *et al.*, Plasma Phys. Control. Fusion **47** (2005) 17

[3] B. Pégourié *et al.*, Nucl. Fusion **47** (2007) 44

[4] R. Wenninger *et al.*, Nucl. Fusion **55** (2015) 063003

This work has been carried out within the framework of the EUROfusion Consortium and has received funding from the Euratom research and training programme 2014-2018 under grant agreement No 633053. The views and opinions expressed herein do not necessarily reflect those of the European Commission.